Temperature Sensitivity of Nanochannel Electrical Conductance

Mojtaba Taghipoor,* Arnaud Bertsch, and Philippe Renaud

Microsystems Laboratory, Ecole Polytechnique Federale de Lausanne, EPFL STI-IMT-LMIS, Station 17, 1015 Lausanne, Switzerland

ABSTRACT Electrical measurement is a widely used technique for the characterization of nanofluidic devices. The electrical conductivity of electrolytes is known to be dependent on temperature. However, the similarity of the temperature sensitivity of the electrical conductivity for bulk and nanochannels has not been validated. In this work, we present the results from experimental measurements as well as analytical modeling that show the significant difference between bulk and nanoscale. The temperature sensitivity of the electrical conductance of nanochannel is higher at low ionic concentration where the nanofluidic transport is governed by the electrostatic effects from the wall. Neglecting this effect can result in significant errors for high temperature measurements. Additionally, the temperature sensitivity of the nanochannel conductance allows to measure the enthalpy change of surface reactions at low ionic concentrations.

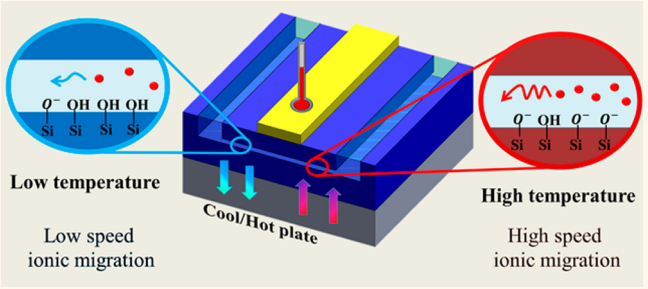

KEYWORDS: nanofluidics · temperature sensitivity · surface charge density · electrical conductance · enthalpy change

Optical observation of molecular transport, such as using fluorescently dyed molecules, is commonly used in nanofluidic studies. However, the electrical characterization is indeed a very complementary method, which also offers the possibility to perform label free measurements on such systems. Characterization of nanofluidic channels,[1−3] single molecule translocation[4] and detection,[5] characterization of nanofluidic field effect transistors[6,7] and diodes[8,9] and estimation of fluid temperature by electrical conductance measurement[10] are some of the reported applications that used the electrical measurements in nanofluidic studies.

The electrical conductivity of an electrolyte depends on its temperature since the mobility of ions changes with temperature. Aqueous solutions show an increase in electrical conductivity with temperature since the decrease of water viscosity makes it easier for the ions to migrate. Different ions have different mobilities and the sensitivity of their mobility to temperature change is different,[11] too. The evolution of the electrical conductivity of different solutions with temperature has been studied by many research groups and reported to raise with temperature.[12]

Moreover, the electrical conductance of nanochannels is known to differ from the bulk due the distinctive effect of nanochannel wall that is electrostatically charged.[1−3,6,8] The electrostatic field induced by the charges carried by the wall (wall electrostatic field) leads to a charged layer called electric double layer (EDL), where the concentration of counterions is more than the bulk and this extra concentration makes the nanochannel more conductive than the bulk. Despite many studies focused on modeling and testing the influence of the wall effect on the electrical conductance,[13−15] less attention has been devoted to the study of the influence of temperature change on the nanochannel conductance. Failing to understand how the electrical conductance depends on temperature will result in errors in all related applications. Is the temperature sensitivity of nanochannel conductance similar to the bulk? That is the main question we try to answer in this work.

RESULTS AND DISCUSSION

A set of temperature sensor embedded nanochannels was designed and fabricated as described in Materials and Methods and shown in Figure 1a. The device consists of

* Address correspondence to mojtaba.taghipoor@epfl.ch.

Received for review February 22, 2015 and accepted April 6, 2015.

Published online April 06, 2015
10.1021/acsnano.5b01196

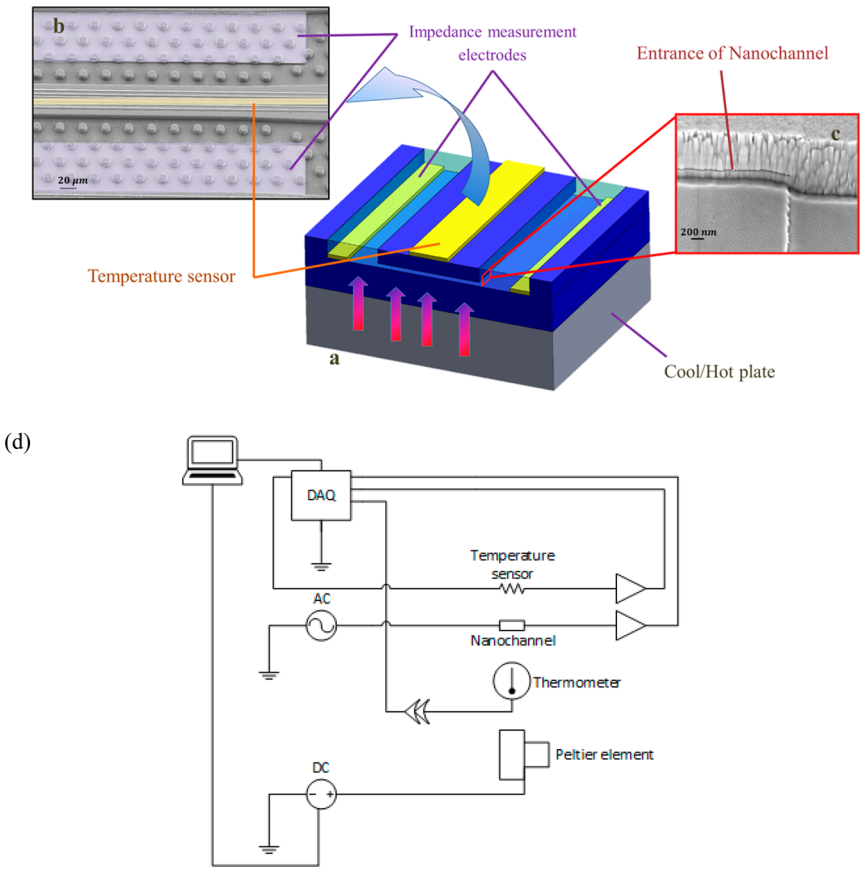

Figure 1. (a)Schematic view of the experimental setup and the fabricated device. The temperature of the device is set by controlling the temperature of a mini cool/hot plate. The nanochannel temperature is measured by a platinum electrode that is integrated 500 nm apart from the nanochannel wall. Two platinum electrodes are used for the nanochannel impedance measurements. Scanning electron micrograph (SEM) of the fabricated device is shown in (b) top view and (c) 30° tilted view of the entrance of a nanochannel. The impedance measurement electrodes are colored in purple and the temperature sensor in yellow. (d) Schematic view of the measurement setup. The nanochannel conductance and temperatures are calculated in a LabVIEW interface using the data acquired by a data acquisition card (DAQ).

two microelectrodes close to the nanochannel openings for measuring the electrical conductance of nanochannel and a thin platinum electrode that was calibrated and used as a nanochannel temperature sensor. The device was then mounted on a temperature controlled mini cool/hot plate and the electrical conductance of nanochannel was measured at different temperatures. The schematic view of the measurement setup is shown in Figure 1d and explained in detail in Materials and Methods.

The electrical conductance of the nanochannel was measured at a temperature range of 5−38 °C. The variation of nanochannel conductance with temperature was then observed at different ionic concentrations. Figure 2 depicts the variation of the normalized nanochannel electrical conductance *versus* temperature at different ionic concentrations. The conductance was normalized to its value at 10 °C. The electrical conductance of nanochannel increases about 3.4 times at 100 μM, while its increase at 1 M is only 1.5 times for the same temperature change of 25 °C.

It is widely known that the electrical conductivity of an electrolyte varies with temperature, which is the

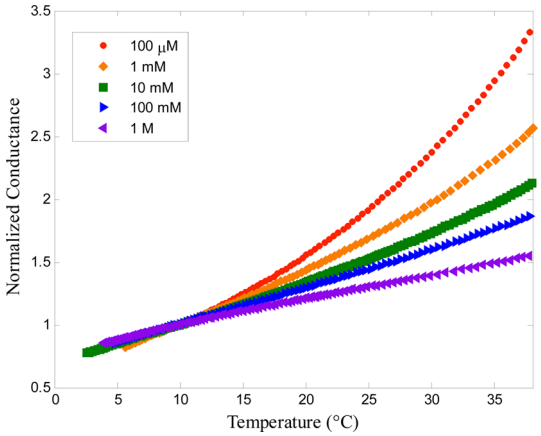

Figure 2. Evolution of normalized electrical conductance of a 45 nm height nanochannel *versus* temperature at different concentrations. At low ionic concentration, the electric conductance of nanochannel is more sensitive to temperature change. The conductance is normalized relative to its value at 10 °C for all ionic concentrations.

case for a nanofluidic channel according to Figure 2. In addition, the temperature sensitivity of electrical conductivity of aqueous solutions varies slightly with ionic

concentration.[16] The question that remains to be answered is that why the temperature sensitivity of nanochannel electric conductance is quite different at different ionic concentrations.

At first glance, this can be related to the electric double layer (EDL) effect, which is the cause of dissimilarities among different nanofluidic transport regimes. The electrical conductivity of aqueous solutions is related to the number density of ions n_i and their electrical mobility μ_i. The number density of an ion inside a nanochannel can be different from the bulk's one depending on the ionic strength of the solution. At higher ionic strength where the electric double layer (EDL) is thin, the number density of ions inside the channel is similar to the bulk whereas it can be several times higher at low ionic strength due to EDL overlap. Thus, at high ionic strength, the variation of electrical conductance with temperature should be more similar to the bulk while it can be different at low ionic strength. At low ionic strength, the number density is a function of the wall surface charge whose temperature dependence will influence the variation of the electric conductance with temperature.

A detailed discussion about the influence of temperature on the wall surface charge and the electrical conductance of nanochannels is required. In the next paragraphs, we use the analytical modeling to study the effect of temperature on nanofluidic transport.

The nanochannel conductance can be written as a superposition of a bulk conductance term G_B and a surface conductance term G_S.[2,3]

$$G_B = e\frac{wh}{d}\sum_i \mu_i n_i \tag{1}$$

$$G_S = 2\mu_e\frac{w}{d}\sigma_n \tag{2}$$

where e, w, h and d are the electron charge, nanochannel width, height, and length, respectively. The two parameters σ_n and μ_e are the charge per surface area (in brief, charge density) and the effective ionic mobility inside the nanochannel, which were defined and discussed in our previous paper.[3] In brief, the charge density σ_n is the net ionic charge inside the nanochannel per surface area, which depends on ionic concentration, pH of the solution and temperature. The effective ionic mobility μ_i is the concentration weighted average of the ionic mobility of all ions presented inside the nanochannel including H^+ and OH^- ions.

For high ionic concentrations, G_B is dominant and the only parameter that depends on temperature is the ionic mobility. Therefore, for a symmetric electrolyte, the temperature sensitivity of the electrical conductance α_{G_B} at neutral pH can be written as

$$\alpha_{G_B} = \frac{1}{\sum\mu_i}\frac{\partial\sum\mu_i}{\partial T} \tag{3}$$

The term "temperature sensitivity" of a variable v is defined mathematically as its relative rate of change with respect to temperature difference ($\alpha_v \equiv (1/v)(\partial v/\partial T)$). As mentioned before, α_{G_B} is known thanks to several works on conductivity meter calibrations. For instance, the temperature sensitivity of potassium chloride solutions has been studied by many research groups and reported to raise between 1.8 and 2% per degree Celsius at room temperature.[12]

On the other hand, at low ionic concentrations where the surface effect is dominant and the EDL is overlapped inside the nanochannel, the temperature sensitivity has an extra term. This means that the temperature sensitivity of the electrical conductance can be different from the bulk which seems to be in line with our measurements of Figure 2.

$$\alpha_{G_S} = \frac{1}{\mu_e}\frac{\partial\mu_e}{\partial T} + \frac{1}{\sigma_n}\frac{\partial\sigma_n}{\partial T} = \alpha_{\mu_e} + \alpha_{\sigma_n} \tag{4}$$

The extra term α_{σ_n} is directly related to the wall surface charge σ_s, which is an explicit function of temperature according to the site binding model developed by Yate *et al.*[17]

$$\sigma_s = e\Gamma_s\frac{K_+[H_B^+]\exp\left(\frac{-e\varphi_0}{k_BT}\right) - \frac{K_-}{[H_B^+]}\exp\left(\frac{e\varphi_0}{k_BT}\right)}{1 + K_+[H_B^+]\exp\left(\frac{-e\varphi_0}{k_BT}\right) + \frac{K_-}{[H_B^+]}\exp\left(\frac{e\varphi_0}{k_BT}\right)} \tag{5}$$

where K_- and K_+ are the equilibrium constants of the reactions occur at the wall surface-electrolyte interface. In the mentioned equation, the surface charge is a function of an unknown electric potential and the system needs more equations to be determined. Subsequently, some more temperature dependent parameters contribute to determination of surface charge density. Moreover, the equilibrium constants as well as the wall electric potential are functions of temperature, which makes the problem more complicated.

Some temperature dependent parameters that can play a role in electrical conductance of a nanochannel are introduced in Table 1. We discuss about these parameters in the following paragraphs and use them in the calculation of surface charge density of a nanochannel wall.

Equilibrium Constant. The rate of chemical reactions is significantly influenced by temperature variation. The nanochannel wall reactions are not exceptions. The equilibrium constant K_{eq} of a reaction is related to the standard Gibbs free energy of the reaction ΔG° and absolute temperature T via

$$\Delta G^\circ = -RT\ln K_{eq} \tag{6}$$

where R is the gas constant. Using the definition of Gibbs free energy and eq 6, the temperature sensitivity of the equilibrium constant is related to the temperature and the standard enthalpy change of the reaction

TABLE 1. Temperature Sensitivity of Important Physical Parameters

parameter (p)	relationship	α_p (%)
Equilibrium constant K	$\Delta G^\circ = -RT \ln K_{eq}$	2−12
Ionic mobility μ_i	$\mu_i = \frac{\lvert z_i \rvert e}{6\pi r_i \eta(T)}$	2.1
Dielectric constant ϵ_f	Malmberg and Maryott[23]	−0.45
Thermal voltage V_T	$V_T = \frac{k_B T}{e}$	0.3
Debye length λ_D	$\lambda_D = \left(\frac{\epsilon_f \epsilon_0 k_B T}{2e^2 I}\right)^{1/2}$	−0.06

ΔH° *via* Van't Hoff equation.

$$\alpha_{K_{eq}} = \frac{\Delta H^\circ}{RT^2} \tag{7}$$

In this equation, the enthalpy and entropy change of the reaction are assumed constant, which is a correct approximation in the small temperature ranges.[18]

As for many nanofluidic devices, the enthalpy change of reaction of a silica surface has been reported to be in the range of $\Delta H^\circ = -15$ kJ mol^{-1} to $\Delta H^\circ = -90$ kJ mol^{-1}.[19] Hence, the temperature sensitivity of the equilibrium constant at room temperature will be in the range of $\alpha_{K_{eq}} = 2\%$ to $\alpha_{K_{eq}} = 12\%$. This relatively high temperature sensitivity implies that the electrical conductance of the nanochannel will be different from the bulk when it is determined by the wall surface charge.

Since the number of binding sites that contribute to the surface reactions depends on the pH value, the enthalpies of surface reactions might be pH dependent, too. Some groups[20,21] reported the dependency of enthalpies of the surface reactions on the pH for different metal oxides. Some others measured the enthalpy of surface reactions only at the point of zero charge (PZC)[22] since the measurements outside the PZC region cannot simply be justified by normal stoichiometric calculations. In fact, the enthalpy change of surface reactions can be expressed as a summation of the standard and the electrostatic contributions.[21] As far as the temperature variation can change the electrostatic properties of the surface, the enthalpy change of the surface reactions might be dependent on temperature, too. In this work, the enthalpy change of surface reactions of silicon dioxide was assumed constant since the temperature range is small. However, different enthalpies can be utilized at different pH values.

Ionic Mobility. The ionic mobility μ_i (m^2 V^{-1} s^{-1}) of an ion i is defined as its traveling velocity when a unit electric field applies. It can be expressed as

$$\mu_i = \frac{\lvert z_i \rvert e}{6\pi r_i \eta} \tag{8}$$

where z_i, e, r_i and η are the charge number of ith ion, the electron charge, the ionic radius of ith ion, and the dynamic viscosity of the electrolyte, respectively. Since the viscosity of water decreases by increasing the temperature,[12] the ionic mobility of solvated ions and consequently the conductivity of water increases. The temperature sensitivity of water dynamic viscosity is $\alpha_\eta = -2.1\%$[12] and subsequently, the temperature sensitivity of ionic mobility is $\alpha_{\mu i} = 2.1\%$. The temperature sensitivity of the ionic mobility is the cause of the electrical conductance variations in bulk regimes according to eq 3.

Electric Permittivity. The electric permittivity of liquid water is known to decrease by increasing the temperature.[12,23,24] The relationship suggested by Malmberg and Maryott[23] was used here to calculate the temperature sensitivity of the electric permittivity which is given as

$$\epsilon = 87.740 - 0.40008\theta + 9.398(10^{-4})\theta^2 - 1.410(10^{-6})\theta^3 \tag{9}$$

where θ is the temperature in degrees Celsius. The temperature sensitivity is then $\alpha_\epsilon = -0.45\%$ at 25 °C.

Dissociation Constant of Water. Autoprotolysis of water and its dependence to the electric field was studied numerically for a nanofluidic field effect transistor.[13] Like any chemical reaction, the dissociation of water molecule is temperature dependent and should be considered in our study. At low ionic concentrations where the salt concentration is of the same order as the ionized water molecule concentration (*i.e.*, H^+ and OH^- concentration) considering self-ionization of water is necessary. Specially, in surface chemistry studies, as the surface charge is strongly influenced by the pH, neglecting the self-ionization of water can result in errors. Additionally, the ionization of water, like any other chemical reaction, is temperature dependent and its dissociation constant pK_w decreases by increasing the temperature.[12] Although the temperature sensitivity of pK_w is very small, its variation with temperature is taken into account in our modeling since the wall surface charge is strongly dependent on the pH value of the solution.

Thermal Voltage. The thermal voltage is an expression of the thermal energy of ions in the solution in terms of the electric potential. It is related to the absolute temperature T and the electron charge e *via*

$$V_T = \frac{k_B T}{e} \tag{10}$$

where k_B is the Boltzmann constant. It influences the ionic distribution toward the wall and since it is

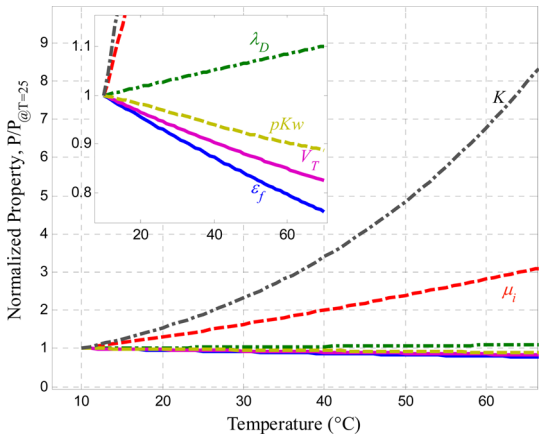

Figure 3. Normalized physical properties value *versus* temperature. The increase of the equilibrium constant K (Black dash-dot line) and the ionic mobility μ_i (red dashed line) are more dominant than other properties. In equilibrium constant calculations, the enthalpy change of the reaction was assumed constant and equal to $\Delta H^\circ = -30$ kJ mol^{-1}. The inset shows a zoomed view of the changes of Debye length λ_D (green dash-dot), dissociation constant of self-ionization of water pK_w (yellow dashed), thermal voltage V_T (pink solid line) and the relative permittivity of water ε_f (blue solid line).

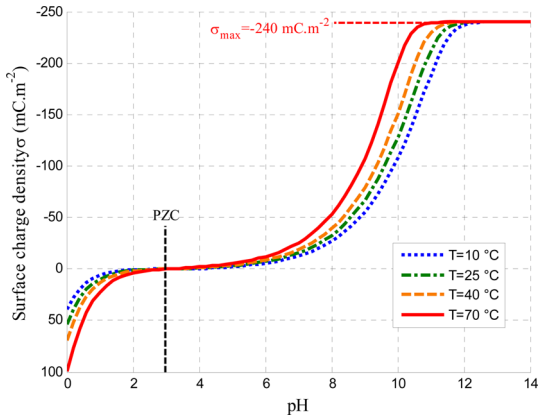

Figure 4. Evolution of modeled surface charge density *versus* pH for a silicon dioxide surface (pK_- = −6.3, N_s = 1.5 site·nm^{-2}, $\Delta H^\circ = -30$ kJ mol^{-1}) at 1 mM concentration of potassium chloride. The red solid line (T = 70 °C), the orange dashed line (T = 40 °C), the green dash-dot line (T = 25 °C) and the blue dotted (T = 10 °C) show how the wall surface charge changes at different temperatures. The higher temperature of electrolyte leads to a higher magnitude of surface charge density.

explicitly related to the temperature, its variation with temperature can influence the nanochannel electrical conductance. At room temperature, the thermal voltage is about $V_T \approx 26$ mV which is in the same order of magnitude as the wall electric potential for a silica surface in normal conditions. Its temperature sensitivity is $\alpha_{V_T} = 1/T$, which is about 0.3% at room temperature.

Debye Length. The Debye length is a characteristic length that depends on the thermal energy and ionic strength of the solution and is independent of the wall electric field.

$$\lambda_D = \left(\frac{\epsilon_f \epsilon_0 k_B T}{2e^2 I}\right)^{1/2} \quad (11)$$

where ϵ_f, ϵ_0 and I are the relative dielectric constant of electrolyte, dielectric constant of vacuum and the ionic strength of the solution, respectively. Its temperature sensitivity can be expressed as a function of α_ϵ and α_{V_T}. The relative rate of change of the Debye length can then be expressed as

$$\alpha_{\lambda_D} = \frac{1}{2}(\alpha_\epsilon + \alpha_{V_T}) \quad (12)$$

According to the estimated values, its temperature sensitivity is $\alpha_{\lambda_D} = -0.06\%$, which is relatively low. This means that temperature has a minor effect on the screening length of the wall electric field.

Figure 3 compares the normalized values of the mentioned parameters in a temperature range of 10 to 70 °C. All the values are normalized by dividing by their value at room temperature. As it is depicted, the increase of the equilibrium constant K and the ionic mobility μ_i are dominant. It means that increasing the temperature will increase the electrical conductance *via* the ionic mobility increase. Likewise, increasing the temperature changes the electrical conductance by changing the wall surface charge as discussed before. However, according to the analytical modeling of the electrical conductance, having high temperature sensitivity of a parameter does not necessarily show a significant impact of that parameter on the temperature sensitivity of the electrical conductance.

Taking into account the temperature dependency of mentioned variables, the surface charge density of a silica nanochannel wall was calculated in a temperature range of 0 to 70 °C using the analytical modeling suggested in our previous work.[3] Figure 4 shows the evolution of calculated surface charge density *versus* pH at different temperatures. A higher temperature of the electrolyte leads to a higher magnitude of surface charge density. It means that the additional term in eq 4 should not be neglected. There is an exceptional case when all the binding sites of the surface are charged. In this condition, the temperature will not have any effect like the situation of the maximum surface charge density at high pH values.

Additionally, the point of zero charge (PZC) may be shifted to the right or left if the values of enthalpy change of the surface reactions are different.

$$\frac{\partial pH_{PZC}}{\partial T} = -\frac{1}{2RT}(\Delta H_-^\Theta - \Delta H_+^\Theta) \quad (13)$$

The PZC shift with temperature change was observed previously and reported to approach the neutral point with increasing the temperature for a TiO_2 surface.[25]

As it is shown in the inset of Figure 5, the variation of surface charge density has a direct impact on the wall electric potential. Some studies in surface chemistry[26]

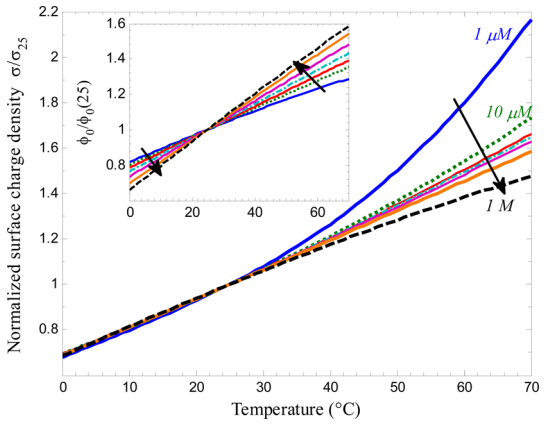

Figure 5. Change in normalized surface charge density σ/σ_{25} and normalized wall electric potential $\varphi_0/\varphi_{0_{25}}$ (inset) *versus* temperature at 1 μM (blue line), 10 μM (green dotted), 100 μM (red solid line), 1 mM (cyan dash-dot), 10 mM (pink solid), 100 mM (orange solid) and 1 M (black dashed) potassium chloride concentrations at pH = 7. The graph shows that the magnitude of surface charge and electric potential increase with increasing the temperature despite different slopes at different concentrations. The arrows show the increase of ionic concentration direction.

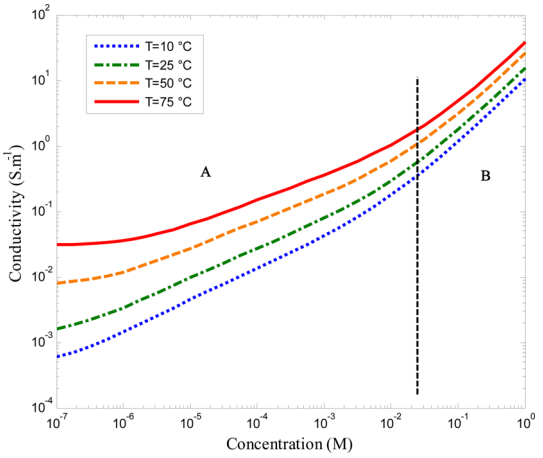

Figure 6. Calculated conductivity change *versus* salt concentration at T = 75 °C (red solid line), T = 50 °C (orange dashed), T = 25 °C (green dash-dot) and T = 10 °C (blue dotted). It is obvious that the change of conductivity with temperature is higher at low ionic concentrations (region A) where it is governed by the wall surface charge. At high concentrations (region B), a smaller increase of conductivity is still observable since the ionic mobility of water increases with temperature too. The solution is considered to be at pH = 7 and the nanochannel surface is silicon dioxide ($pK_- = -6.3$, N_s = 1.5 site·nm^{-2}, $\Delta H° = -30$ kJ mol^{-1}).

and geophysics[19,27] and recently in microfluidics[28,29] studied the effect of temperature change on the zeta potential for different surface types. Generally, the magnitude of the zeta potential has been reported to increase by increasing the temperature for the case of a silica surface. In the present analytical modeling, as Figure 5 shows, the magnitude of the wall electric potential increases with temperature, too. It shows that normalized surface charge density σ_0 and stern layer potential φ_0 have positive slopes with respect to temperature increase.

The variation of surface charge density is not similar at all ionic concentrations. At low ionic concentration, the surface charge density is more sensitive to temperature change. Contrarily, the slopes of high ionic concentration curves are lower for the electric potential of the nanochannel wall. The dependency of temperature sensitivity of both surface charge and electric potential to concentration implies that the temperature sensitvity of nanochannel electrical conductance can also be related to the concentration.

Considering the concentration dependency of surface charge variation with temperature and taking into account all the temperature dependent variables, the analytical model was used to calculate the average electrical conductivity of the solution (what we call "nanochannel conductivity") inside a 35 nm height nanochannel at different concentrations. As it is shown in Figure 6, a temperature rise makes the nanochannel more conductive. That is due to the known fact that water conductivity increases by increasing the temperature (region B), which is related to the change in the ionic mobility of salt ions. As expected, the nanochannel is more sensitive to the temperature change at lower concentrations (region A) since the effect of wall surface charge adds up to the bulk conductance variation. This is the key point that has not been considered in previous nanofluidic studies. The conductance increases more than 1 order of magnitude for a temperature rise of 65 °C at ionic concentrations lower than 1 mM. The conclusion is that the nanofluidic transport at EDL overlapped condition is influenced by temperature in a different way, as it is depicted in Figure 7. At low temperature, the silica surface of nanochannel is less charged and less number of ions can pass. At high temperature, the surface charge is higher, the concentration of counterions increases inside the channel, the water is less viscous and consequently, the ionic transport occurs faster.[30−32] This results imply that for the case of thermally nanoactuated macromolecular gates,[30−32] the temperature sensitivity of wall surface charge should be taken into account. Specially, for the case of small pore diameter nanoconduit whose electrical conductance is governed by the wall surface charge, the role of wall surface charge is not ignorable. Additionally, this significant change of nanochannel conductivity, especially at low concentrations, provides the possibility of modulating the nanofluidic transport by means of temperature change.

We also investigated the temperature sensitivity experimentally. As presented in Figure 8, the slope of the normalized conductance is higher at low concentrations and both experimental and analytical results are consistent. The enthalpy change of surface reactions for a silicon dioxide surface was taken $\Delta H° = -40$ kJ mol^{-1} in analytical calculations. According to this figure, because of the nonequal temperature sensitivity of nanochannel conductance at different

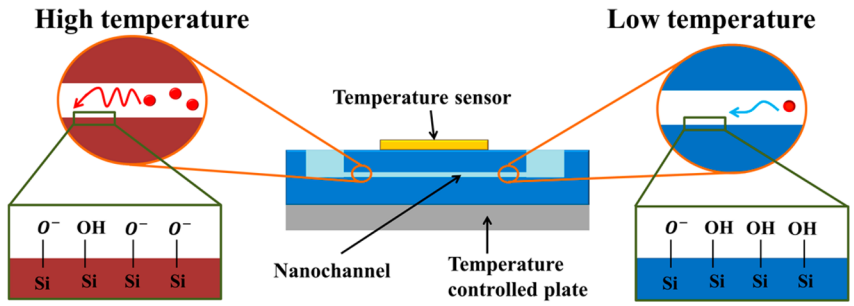

Figure 7. Schematic explanation of the temperature effect on the electrical conductance of nanochannel. At low temperature, the silica surface of nanochannel is less charged and less number of ions can pass. At high temperature, the surface charge is higher, the concentration of counterions increases inside the channel, the water is less viscous, and consequently, the ionic transport occurs faster.

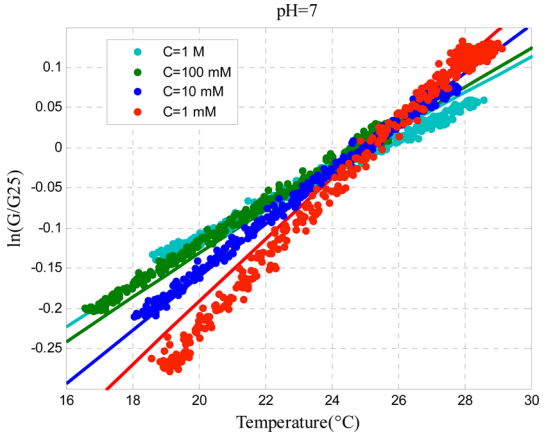

Figure 8. Evolution of natural logarithm of normalized conductance ($\ln(G/G_{25})$) from the measurements *versus* temperature at c = 1 M (cyan circles), c = 100 mM (green circles), c = 10 mM (blue circles) and c = 1 mM (red circles). The colored lines are the modeled conductance for a silicon dioxide surface ($\Delta H° = -40$ kJ mol^{-1}). The slopes show the temperature sensitivity of the electrical conductivity.

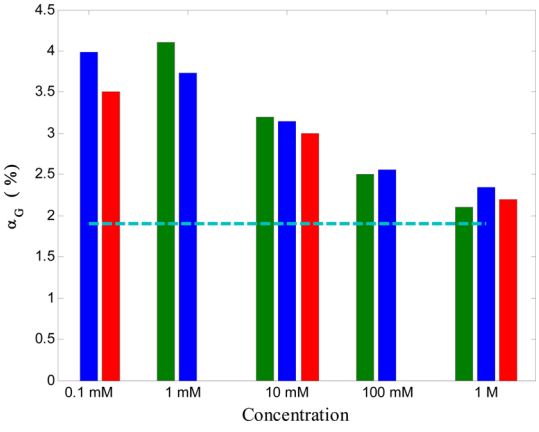

Figure 9. Comparison of temperature sensitivity of measured electrical conductivity (red and green bars show different devices) with analytical model (blue bars) and bulk value (cyan dashed line) at room temperature. The measured temperature sensitivity is higher at low ionic concentrations where the conductivity is governed by the wall surface charge.

concentrations, different sensitivities should be specified for the applications that use the electrical conductance measurement to estimate the temperature inside the nanochannel.[10]

Figure 9 illustrates the temperature sensitivity of the nanochannel conductance at different ionic concentrations. It compares the experimental results for two devices of different geometries with the model. It clearly proves that when the surface charge is the main factor in conductance calculation, the temperature sensitivity of the conductance is higher. According to the measured temperature sensitivity, an experimental measurement with only two degrees Celsius of temperature difference will have more than 8% error at low concentrations, which should be noticed in all of the nanofluidic applications that use the electrical measurements for characterization, sensing or any other purposes. The bulk temperature sensitivity was also evaluated using the same experimental setup. The result is 1.9%, which is consistent with the known value from the literature.[12] In analytical modeling, the enthalpy change value was selected to be $\Delta H° = -40$ kJ mol^{-1} for silicon dioxide surface. As mentioned before, the enthalpy change of silicon dioxide surface reaction has been reported to be between -15 and -90 kJ mol^{-1}.[19] The higher enthalpy change results in higher temperature sensitivity of electrical conductance at low concentrations as it is shown in Figure 10. In this figure, the modeled temperature sensitivity of the nanochannel electrical conductance for different enthalpy changes is compared with the measured data for two different devices. According to the model, the temperature sensitivity is higher at low concentrations for all enthalpies. At high ionic concentrations, on the other hand, the values are lower, close to the bulk values and independent from the enthalpy change, which confirms the independency of temperature sensitivity from the surface. Comparing the experimental data and the model provides the possibility of measuring the enthalpy change of surface reactions. Although calorimetry as the conventional method is normally used to measure the enthalpy of surface reactions,[21] this can also be introduced as a new method for measuring the enthalpy change of metal oxide surface

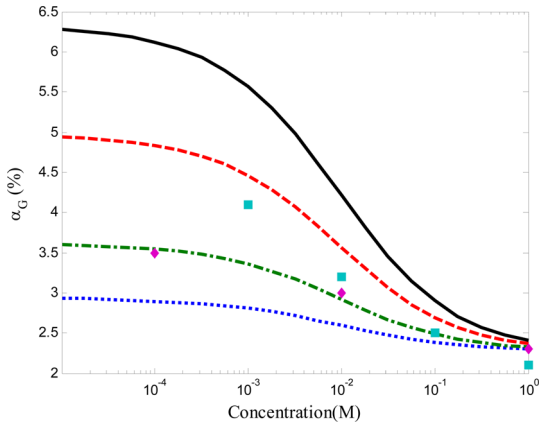

Figure 10. Comparison of the measured temperature sensitivity of the electrical conductivity with the results from the model for $\Delta H° = -90$ kJ mol^{-1} (black solid line), $\Delta H° = -60$ kJ mol^{-1} (red dashed), $\Delta H° = -30$ kJ mol^{-1} (green dash-dot) and $\Delta H° = -15$ kJ mol^{-1} (blue dotted). The higher enthalpy change of the surface reaction leads to a higher temperature sensitivity at low ionic concentrations. Cyan squares and magnetite diamonds represent the experimental data for two different devices. The devices are of the same height but different width and length. Two devices are also different in terms of surface properties that can be the result of processing uncertainties and different number and type of adsorbed ions on the nanochannel wall.

reactions at solid-electrolyte interface. According to our model, the enthalpy change is a linear function of α_G and can be easily used for this purpose in nanofluidic studies as well as other related fields like geophysics.

CONCLUSION

The effect of temperature on nanochannel electrical conductance was studied. The surface charge of nanochannel walls depends on temperature, which causes the temperature sensitivity of the nanochannel conductance to be different from the bulk at low ionic concentration. The temperature sensitivity of the electrical conductance is higher at low ionic concentration for a silicon dioxide nanochannel. This implies that using the bulk values of the temperature sensitivity of the electrical conductance in a nanochannel configuration leads to major errors at low ionic concentrations. We measured 8% error for only 2 °C temperature difference at low ionic concentration in a silicon dioxide nanochannel filled with 1 mM potassium chloride solution. This implies that different experiments that use the nanochannel electrical measurements should consider the temperature effect correctly.

The error is more considerable for temperature changes of more than tens of degrees. At this condition, neglecting the nanoscale effects may result in a measurement error of more than 1 order of magnitude at low ionic concentrations. In this situation, using equations that are valid for the bulk should be avoided for equivalent temperature estimations inside the nanochannel.

The modeling predicts more than 1 order of magnitude increase in nanochannel conductance compared to bulk values for a 60 °C temperature rise. This influence of the temperature on nanochannel conductance suggests a new possibility of nanofluidic transport modulation that we have planned to test.

According to our model, the temperature sensitivity of nanochannels is a strong function of the enthalpy change of surface reaction at low ionic concentrations, which leads to a new method for measuring the enthalpy change of different surface reactions.

MATERIALS AND METHODS

Fabrication. A set of 35 nm height nanochannels was fabricated using the sacrificial layer approach. A 35 nm thick amorphous silicon was sputtered on a fused silica wafer and patterned to define the shape of nanochannels. Then, a 500 nm silicon dioxide layer was deposited using low-pressure chemical vapor deposition (LPCVD) followed by an annealing step. Platinum electrodes were then deposited and patterned using normal photolithography techniques and covered by another low temperature oxide (LTO) layer. The microchannels were then fabricated in the same chip by etching the oxide until the amorphous silicon openings. The amorphous silicon was then etched isotopically and the nanochannels got open. The device was covered by a PDMS part that included the reservoirs.

Two platinum electrodes were embedded close to the openings of the nanochannel for nanochannel impedance measurements.

Experimental Setup. A Peltier element (3.9 A, 37.9 W, Laird) was utilized and controlled by a computer controlled DC power supply (Hewlett-Packard E3631A) in order to set the device temperature. The device was mounted on top of an aluminum adaptor that was in contact with the Peltier and its temperature was controlled easily by controlling the current passing through the Peltier element. A thermocouple was used to provide a temperature feedback, whose data was collected by a data acquisition card DAQ (National Instrument PCI-6251). A computer interface (LabVIEW2013) was used to acquire the data and produce a control command for the power supply.

Temperature Sensor. A platinum electrode that is insulated by a 500 nm silicon dioxide layer was integrated over the nanochannels and calibrated in order to be used as a nanochannel temperature sensor (Figure 1a,b). The temperature was measured using a setup as sketched in Figure 1d. As it is shown in the figure, a function generator applied a relatively low electric potential AC signal to the temperature sensor in order to eliminate the Joule heating and electrostatic effects. The current was converted to voltage, which was read by DAQ. The resistance of the platinum electrode was then calculated at different temperatures and calibrated for measuring the nanochannel temperature.

Impedance Measurement. The impedance of nanochannel was measured at different frequencies using an impedance analyzer (Agilent 4294A precision impedance analyzer). The impedance spectrum was then analyzed to find the right frequency where the impedance corresponds to the nanochannel resistance. The nanochannel resistance corresponds to the impedance where the phase is closest to zero, according to the equivalent electric circuit of the nanochannel.

For the case of nanochannel impedance measurement, a similar electric circuit as for the electrode was used. The only difference was a low noise current preamplifier that was used in nanochannel impedance measurements since the current is very small and can be disturbed by different noises that may be present. The whole experiment was conducted inside a Faraday cage having the same ground as all the equipment.

Conflict of Interest: The authors declare no competing financial interest.

Acknowledgment. The authors acknowledge valuable support from CMI (Center of MicroNanoTechnology) for their support and advice during device fabrication specially Cyrille Hibert, Philippe Langlet, Joffrey Pernollet and Anthony Guillet. The authors thank David Bonzon, Guillaume Petitpierre and Nicolas Uffer for kind help in experimental setup fabrication and Damien Pidoux for helpful discussions.

REFERENCES AND NOTES

1. Stein, D.; Kruithof, M.; Dekker, C. Surface-Charge-Governed Ion Transport in Nanofluidic Channels. *Phys. Rev. Lett.* **2004**, *93*, 035901.
2. Schoch, R. B.; Renaud, P. Ion Transport through Nanoslits Dominated by the Effective Surface Charge. *Appl. Phys. Lett.* **2005**, *86*, 253111.
3. Taghipoor, M.; Bertsch, A.; Renaud, P. An Improved Model for Predicting Electrical Conductance in Nanochannels. *Phys. Chem. Chem. Phys.* **2015**, *17*, 4160–4167.
4. Steinbock, L. J.; Bulushev, R. D.; Krishnan, S.; Raillon, C.; Radenovic, A. DNA Translocation through Low-Noise Glass Nanopores. *ACS Nano* **2013**, *7*, 11255–11262.
5. Raillon, C.; Cousin, P.; Traversi, F.; Garcia-Cordero, E.; Hernandez, N.; Radenovic, A. Nanopore Detection of Single Molecule RNAP−DNA Transcription Complex. *Nano Lett.* **2012**, *12*, 1157–1164.
6. Karnik, R.; Fan, R.; Yue, M.; Li, D. Y.; Yang, P. D.; Majumdar, A. Electrostatic Control of Ions and Molecules in Nanofluidic Transistors. *Nano Lett.* **2005**, *5*, 943–948.
7. Wu, S.; Wildhaber, F.; Bertsch, A.; Brugger, J.; Renaud, P. Field Effect Modulated Nanofluidic Diode Membrane Based on Al2O3/W Heterogeneous Nanopore Arrays. *Appl. Phys. Lett.* **2013**, *102*, 213108.
8. Wu, S.; Wildhaber, F.; Vazquez-Mena, O.; Bertsch, A.; Brugger, J.; Renaud, P. Facile Fabrication of Nanofluidic Diode Membranes Using Anodic Aluminium Oxide. *Nanoscale* **2012**, *4*, 5718–5723.
9. Karnik, R.; Duan, C.; Castelino, K.; Daiguji, H.; Majumdar, A. Rectification of Ionic Current in a Nanofluidic Diode. *Nano Lett.* **2007**, *7*, 547–551.
10. Jonsson, M. P.; Dekker, C. Plasmonic Nanopore for Electrical Profiling of Optical Intensity Landscapes. *Nano Lett.* **2013**, *13*, 1029–1033.
11. Sluyters, J. H.; Sluyters-Rehbach, M. Temperature Dependence of the Properties of Water and Its Solutes, Including the Supercooled Region. *ChemPhysChem* **2013**, *14*, 3788–3800.
12. W. M. Haynes *CRC Handbook of Chemistry and Physics*, 95th ed.; Revised; Apple Academic Press Inc.: Oakville, 2014.
13. Pardon, G.; van der Wijngaart, W. Modeling and Simulation of Electrostatically Gated Nanochannels. *Adv. Colloid Interface Sci.* **2013**, *199−200*, 78–94.
14. Yeh, L.-H.; Xue, S.; Joo, S. W.; Qian, S.; Hsu, J.-P. Field Effect Control of Surface Charge Property and Electroosmotic Flow in Nanofluidics. *J. Phys. Chem. C* **2012**, *116*, 4209–4216.
15. Baldessari, F.; Santiago, J. G. Electrophoresis in Nanochannels: Brief Review and Speculation. *J. Nanobiotechnol.* **2006**, *4*, 12.
16. Katayama, S. Conductimetric Determination of Ion-Association Constants for Calcium, Cobalt, Zinc, and Cadmium Sulfates in Aqueous Solutions at Various Temperatures between 0 °C and 45 °C. *J. Solution Chem.* **1976**, *5*, 241–248.
17. Yates, D. E.; Levine, S.; Healy, T. W. Site-Binding Model of the Electrical Double Layer at the Oxide/water Interface. *J. Chem. Soc., Faraday Trans. 1* **1974**, *70*, 1807–1818.
18. Atkins, P.; de Paula, J. *Elements of Physical Chemistry*; OUP: Oxford, 2013.
19. Reppert, P. M.; Morgan, F. D. Temperature-Dependent Streaming Potentials: 1. Theory. *J. Geophys. Res. Solid Earth* **2003**, *108*, 2546.
20. Machevsky, M. L.; Anderson, M. A. Calorimetric Acid-Base Titrations of Aqueous Goethite and Rutile Suspensions. *Langmuir* **1986**, *2*, 583–587.
21. Kallay, N.; Preočanin, T.; Žalac, S.; Lewandowski, H.; Narres, H. D. Electrostatic Contribution to the Enthalpy of Charging at Hematite/Electrolyte Interface. *J. Colloid Interface Sci.* **1999**, *211*, 401–407.
22. De Keizer, A.; Fokkink, L. G. J.; Lyklema, J. Thermodynamics of Proton Charge Formation on Oxides. Microcalorimetry. *Colloids Surf.* **1990**, *49*, 149–163.
23. Malmberg, C. G.; Maryott, A. A. Dielectric Constant of Water from 0° to 100° C. *J. Res. Natl. Bur. Stand. (U.S.)* **1956**, *56*, No. 2641.
24. Kaatze, U. The Dielectric Properties of Water in Its Different States of Interaction. *J. Solution Chem.* **1997**, *26*, 1049–1112.
25. Bérubé, Y. G.; de Bruyn, P. L. Adsorption at the Rutile-Solution Interface: I. Thermodynamic and Experimental Study. *J. Colloid Interface Sci.* **1968**, *27*, 305–318.
26. Revil, A.; Pezard, P. A.; Glover, P. W. J. Streaming Potential in Porous Media: 1. Theory of the Zeta Potential. *J. Geophys. Res. Solid Earth* **1999**, *104*, 20021–20031.
27. Reppert, P. M.; Morgan, F. D. Temperature-Dependent Streaming Potentials: 2. Laboratory. *J. Geophys. Res. Solid Earth* **2003**, *108*, 2547.
28. Venditti, R.; Xuan, X.; Li, D. Experimental Characterization of the Temperature Dependence of Zeta Potential and Its Effect on Electroosmotic Flow Velocity in Microchannels. *Microfluid. Nanofluidics* **2006**, *2*, 493–499.
29. Hsu, J.-P.; Tai, Y.-H.; Yeh, L.-H.; Tseng, S. Importance of Temperature Effect on the Electrophoretic Behavior of Charge-Regulated Particles. *Langmuir* **2012**, *28*, 1013–1019.
30. Yameen, B.; Ali, M.; Neumann, R.; Ensinger, W.; Knoll, W.; Azzaroni, O. Ionic Transport Through Single Solid-State Nanopores Controlled with Thermally Nanoactuated Macromolecular Gates. *Small* **2009**, *5*, 1287–1291.
31. Guo, W.; Xia, H.; Xia, F.; Hou, X.; Cao, L.; Wang, L.; Xue, J.; Zhang, G.; Song, Y.; Zhu, D.; et al. Current Rectification in Temperature-Responsive Single Nanopores. *ChemPhysChem* **2010**, *11*, 859–864.
32. Nasir, S.; Ali, M.; Ensinger, W. Thermally Controlled Permeation of Ionic Molecules through Synthetic Nanopores Functionalized with Amine-Terminated Polymer Brushes. *Nanotechnology* **2012**, *23*, 225502.